ARTICLE OPEN

Check for updates

Single-cell mapping of peripheral immune dynamics in pregnant women after Moderna mRNA COVID-19 vaccination

Yu-Ting Kang[1], Tsai-Jung Lu[1,2], Po-Liang Cheng[1,3], Li-Wen Lee[1], Pei-Pei Jhan[1], Yi-Ming Chen[1,4,5,6,7,8]✉ and Tzu-Hung Hsiao[1,9,10]✉

Pregnant individuals are at increased risk of severe outcomes from COVID-19 infection, yet the immune responses elicited by vaccination during pregnancy remain poorly understood. In this study, longitudinal single-cell RNA sequencing (scRNA-seq) was performed on peripheral blood mononuclear cells from three pregnant women at four time points: before vaccination, one and two weeks after the first dose of the Moderna mRNA vaccine, and after the second dose postpartum. Dynamic immune changes, including a transient increase in inflammatory classical monocytes (cM_1) after the first dose, marked by elevated expression of IL1B, NLRP3 and NFKB1, as well as moderate activation of interferon-stimulated genes were observed. $CD4^+$ T cells exhibited activation and differentiation into memory subsets. By contrast, B cell responses were minimal after the first dose, and enhanced protein synthesis activity emerged only after the second dose, which suggested delayed humoral activation. Although limited by sample size, our findings indicate that vaccination in pregnancy induces a nonexcessive innate immune activation, coordinated T cell responses and attenuated B cell activity that likely reflect pregnancy-driven immunoregulatory adaptations. These findings reveal the immune dynamics following mRNA vaccination during pregnancy and highlight the importance of developing vaccination strategies tailored for pregnant individuals.

Genes & Immunity (2026) 27:374–383; https://doi.org/10.1038/s41435-026-00394-2

INTRODUCTION

The global COVID-19 pandemic, triggered by the Severe Acute Respiratory Syndrome Coronavirus 2 (SARS-CoV-2), has had profound implications for human health. To date, it has infected more than 700 million people and caused over 6 million deaths globally [1]. Pregnant women are considered a high-risk population due to the unique immune status during pregnancy, which increases their susceptibility to infection, leading to severe health complications and heightened risks for adverse outcomes in infants.

The 2022 updated guidelines from The Centres for Disease Control and Prevention (CDC) regarding pregnant people and COVID-19-related risks states that receiving the COVID-19 vaccine during pregnancy is safe and beneficial [2]. Initially, due to safety concerns, pregnant individuals were excluded from recruitment in various clinical trials, including COVID-19 trials. If pregnancy was detected during the course of a trial, participants were also excluded from receiving additional doses of the vaccine [3]. Subsequent studies have found that pregnant individuals with COVID-19 face higher risks of preterm birth, stillbirth, pre-eclampsia, severe illness, hospitalisation and even death compared with pregnant individuals without COVID-19 [4, 5]. In response, health authorities recommend vaccination during pregnancy as a protective measure. Cohorts from large trials such as the Vaccine Adverse Event Reporting System, v-safe and the Canadian National Vaccine Safety system increasingly show that COVID-19 vaccines do not cause major adverse health events in pregnant individuals or their infants [6, 7]. Although some side effects may occur, they are generally mild and well tolerated.

Although serological studies have confirmed robust antibody production following COVID-19 vaccination, the temporal and cellular immune dynamics, particularly the interplay between innate and adaptive immunity as well as the immunological effect of childbirth in pregnant individuals remain poorly characterised. To address this knowledge gap, single-cell RNA sequencing (scRNA-seq) was performed on peripheral blood mononuclear cells (PBMCs) collected from three pregnant donors at four critical time points: before vaccination, one week and two weeks after the first dose, and after the second dose postpartum. This longitudinal sampling strategy enabled investigating how vaccination and parturition influence immune cell composition, activation states and transcriptional programs during pregnancy. By integrating antibody titres, gene expression profiles and pathway analyses, this study provides valuable insights into vaccine-induced immunomodulation in pregnancy and informs future evaluation of vaccine responses in vulnerable populations.

[1]Departments of Medical Research, Taichung Veterans General Hospital, Taichung, Taiwan. [2]Graduate Institute of Biomedical Electronics and Bioinformatics, National Taiwan University, Taipei, Taiwan. [3]Department of Pathology and Laboratory Medicine, Perelman School of Medicine, University of Pennsylvania, Philadelphia, PA, USA. [4]School of Medicine, College of Medicine, National Yang-Ming Chiao Tung University, Taipei, Taiwan. [5]Division of Allergy, Immunology, and Rheumatology, Department of Internal Medicine, Taichung Veterans General Hospital, Taichung, Taiwan. [6]Department of Post-Baccalaureate Medicine, College of Medicine, National Chung Hsing University, Taichung, Taiwan. [7]Graduate Institute of Clinical Medicine, College of Medicine, National Chung Hsing University, Taichung, Taiwan. [8]Precision Medicine Research Center, College of Medicine, College of Medicine, National Chung Hsing University, Taichung, Taiwan. [9]Department of Public Health, Fu Jen Catholic University, New Taipei City, Taiwan. [10]Institute of Genomics and Bioinformatics, National Chung Hsing University, Taichung, Taiwan. ✉email: ymchen1@vghtc.gov.tw; thsiao@vghtc.gov.tw

Received: 4 January 2024 Revised: 2 February 2026 Accepted: 16 March 2026
Published online: 14 April 2026

MATERIAL AND METHODS

Study participants

This study was approved by the Institutional Review Board of Taichung Veterans General Hospital (IRB Number CF21270A). Three pregnant women receiving two doses of Moderna mRNA-1273 (Spikevax) were enrolled after informed consent. PBMCs were isolated from 8 mL of blood using density-gradient separation.

Anti-SARS-CoV2-IgG detection

IgG antibodies in serum against the receptor-binding domain of the spike protein S1 subunit of SARS-CoV-2 were measured using an electrochemi-luminescence immunoassay following the manufacturer's instructions (Elecsys® Anti-SARS-CoV-2 S assay, Roche Diagnostics, Basel, Switzerland). The measurement range was 0.40–250 U/mL, and < 0.8 and ≥ 0.80 U/mL were recorded as negative and positive, respectively.

Sample preparation and scRNA-seq library construction

This study followed the Chromium Next GEM Single Cell 3′ Reagent Kits v3.1 protocol (10x Genomics CG000388, Rev A, Pleasanton, CA, USA). Cryopreserved PBMCs were thawed at 37 °C for 1 min and then cultured in RPMI with 10% FBS and 10 ng/mL DNase I to prevent aggregation. Each sample was labelled with Cell Multiplex oligos (PN-1000261, 10x Genomics), and up to 14 samples were pooled for loading onto the Chromium Single Cell Instrument. Each channel processed ~49,500 cells and targeted a recovery of 30,000 cells at 1600 cells/μg. Libraries were prepared using Dual Index Plates TT Set A (PN-1000215) and NN Set A (PN-1000243) according to the manufacturer's protocol. Gene expression and Cell Multiplex libraries were combined at a 4:1 ratio and quality-checked using Qsep100. Sequencing was performed on an Illumina NovaSeq 6000 platform with 150 bp paired-end reads.

scRNA-seq data processing and integration

Sequencing data generated from the Chromium 10x Genomics libraries were processed using Cell Ranger Suite v6.0.1 and aligned to the GRCh38 reference genome. Twelve samples were included in two libraries. After barcode demultiplexing and quantification, a Seurat object was created using R package Seurat (v4.0.1). Cells with percent.mt > 10%, nCount > 90%, nFeature < 1% or > 99%, and doublets identified by DoubletFinder were filtered out, and 12,074 single cells were retained. Common genes across datasets were kept using the intersect function. Data were normalised with SCTransform, and dimensionality reduction was performed using PCA and UMAP, followed by clustering with Louvain algorithm. Dataset integration was conducted using SelectIntegrationFeatures, PrepSCTIntegration, FindIntegrationAnchors and IntegrateData functions. Next, the scaled variable gene matrix underwent PCA, and the top 30 principal components were used for clustering and visualisation with RunUMAP.

Top gene identification and cell annotation

In this analysis, cell type prediction and annotation were performed using SingleR with the Blueprint Encode dataset from the celldex package as a reference. The studies by Wen et al. [8], Tong et al. [9] and Chen [10] were also referenced for additional validation of cell identities. Top marker genes were identified using the FindAllMarkers function with the Wilcoxon rank-sum test (*min.pct* = 0.25, *logfc.threshold* = 0.25, *only.pos* = TRUE).

Differentially expressed gene (DEG) analysis and pathway enrichment

Differentially expressed genes (DEGs) between timepoints were identified using the FindMarkers function in Seurat v4.3.0 with the Wilcoxon rank-sum test (*min.pct* = 0.25, *logfc.threshold* = 0.25). Genes with an adjusted p value < 0.05 (Benjamini–Hochberg correction) were considered significant. Gene symbols were converted to Entrez IDs using the bitr function from clusterProfiler v4.6.0 and the *org.Hs.eg.db* annotation. GO enrichment analysis for Biological Process (BP) terms was performed using enrichGO with parameters *keyType* = 'ENTREZID', *ont* = 'BP', *pvalueCutoff* = 0.05 and *qvalueCutoff* = 0.1.

Defining cell state scores

To evaluate cell-level inflammatory and interferon responses, module scores were calculated using the AddModuleScore function in Seurat. Two curated gene sets were used: an inflammatory module containing *IL1B, IL1A, IL6, CXCL8, IL10, IL18, IL12A, IL12B, IL23A, TNF, TNFRSF1A, TNFRSF1B, CCL2, CCL3, CCL4, CCL5, CCL20, CXCL1–3, CXCL8, CXCL10, NFKB1, NFKBIA, RELA, IKBKB, IKBKG, STAT1, STAT3, JAK1, JAK2, MAPK1, MAPK14, MAP3K7, TLR2, TLR4, TLR7, TLR9, NOD1, NOD2, NLRP3, NLRC4, CRP, SAA1, SAA2, PTX3, NOS2, PTGS2, ALOX5, MMP9, PLA2G2A, S100A8–A12, HMGB1, CASP1, CST7, CEBPB, CEBPD, MYD88* and *TRAF6*; and an interferon-stimulated gene (ISG) module including *ISG15, IFIT1–3, MX1, MX2, OAS1–3, RSAD2, IFI6, IFI27, IFI44, IFI44L, IRF7, IRF9, STAT1, STAT2, BST2, TRIM22, GBP1, GBP2, XAF1* and *DDX60*.

Pathway enrichment analysis

scGSVA package (v0.0.23) was used to estimate single-cell pathway activity. Gene set annotations were generated using the buildAnnot function with gene ontology (GO) terms, and pathway scores were computed using the ssGSEA method. The GSVA package was additionally applied to assess gene set variation across cell clusters. Significantly enriched pathways were identified using findPathway, and the top pathways were selected based on adjusted p values and log fold-change. Their average scores were visualised in a heatmap.

Statistical analysis

Statistical analyses were performed using R. Differential expression was evaluated using the Wilcoxon rank-sum test. Adjusted p values were calculated using the Benjamini–Hochberg method. A threshold of adjusted $p < 0.05$ was considered significant.

RESULTS

Vaccination timeline and anti–SARS-CoV-2 IgG antibody response during pregnancy

To capture dynamic changes in immune cell composition and gene expression following COVID-19 vaccination during pregnancy, serum and PBMC samples were collected from three pregnant participants. Serum was used to measure anti–SARS-CoV-2 IgG antibody levels, whilst PBMCs underwent single-cell RNA sequencing. The timeline of sample collection is illustrated in Fig. 1A. All participants received two doses of COVID-19 vaccine during the study period. PBMCs were collected at four timepoints: T1, before vaccination; T2, 6 days after the first dose; T3, 13 days after the first dose; and T4, more than 2 months after the first dose, following the second dose and delivery. Due to delivery timing differences, the sample collection for PG_3 was delayed. Participants' ages ranged from 33 years to 35 years. To evaluate the effectiveness of the COVID-19 vaccination, anti–SARS-CoV-2 IgG concentrations were measured in serum samples collected at four timepoints following vaccination. The results are shown in Fig. 1B. The detection range of the assay was 0.40–250 U/mL. No IgG antibodies were detected at T1 and T2. At T3, the average antibody concentration reached 17.6 U/mL, which indicated a modest increase. By T4, antibody levels reached the upper detection limit (250 U/mL) in all donors. These findings indicate that a single dose of the Moderna mRNA vaccine was insufficient to elicit a robust antibody response within the first week, and only a slight increase was observed by the second week. A substantial antibody response was achieved only after administration of the second dose. Raw IgG concentrations for each donor are shown in Fig. 1B.

Single-cell profiling of PBMCs from vaccinated pregnant donors

To explore pregnancy-associated immune responses to vaccination, scRNA-seq was performed on PBMCs from the three participants. A total of 11,731 cells were analysed and clustered using UMAP after doublet removal with DoubletFinder (Fig. S1A). Sixteen transcriptionally distinct clusters (Fig. S1B) were identified, and the cell types were annotated based on the expression of canonical lineage markers and other cluster-specific upregulated genes. These included monocytes (CD14, FCGR3A and LYZ), T cells (CD3D, CD3E, CD4, CD40LG, CD8A and CD8B), B cells (MS4A1, CD19, CD79A and IGHM), dendritic cells (CLEC4C, LILRA4, TCF4 and IRF7), NK cells (FCGR3A, NKG7, NCAM1, KLRD1 and KLRF1), megakaryocytes (TUBB1 and PF4) and erythrocytes (HBD and

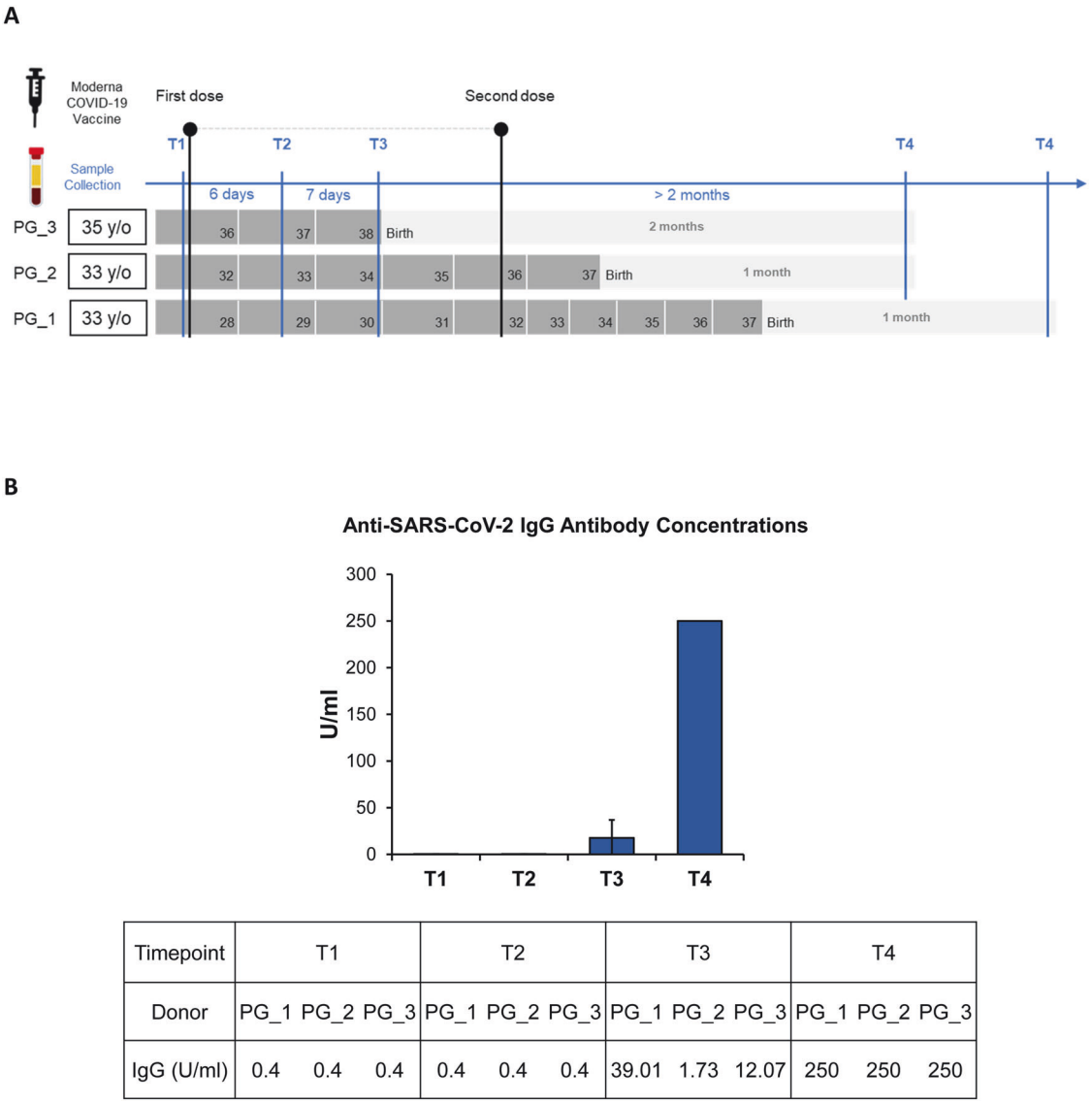

Timepoint	T1			T2			T3			T4		
Donor	PG_1	PG_2	PG_3	PG_1	PG_2	PG_3	PG_1	PG_2	PG_3	PG_1	PG_2	PG_3
IgG (U/ml)	0.4	0.4	0.4	0.4	0.4	0.4	39.01	1.73	12.07	250	250	250

Fig. 1 Study design and anti-SARS-CoV-2 IgG antibody levels in pregnant individuals following COVID-19 vaccination. A Schematic timeline of blood sample collection from three pregnant individuals across four time points during vaccination and postpartum follow-up. **B** Average concentrations of anti-SARS-CoV-2 IgG antibodies (U/ml) across the four time points in the pregnant group.

HBM). These were grouped into 11 canonical immune cell types (Figs. 2A, B). Figure 2C shows the distribution of representative marker genes on the UMAP. Figures S1C and S1D present representative lineage markers and the top 10 highly expressed genes for each cluster. Figure S1E illustrates the UMAP clustering profiles of PBMCs for each donor (top) and across timepoints (bottom), and T4 shows a particularly distinct distribution.

To assess PBMC composition over time, the proportion of each cell type was calculated across timepoints (Fig. 2D), and the average distributions are shown in Fig. 2E. Boxplots indicate that the relative frequencies of all cell types remained largely stable, and no significant changes were observed over time (Fig. 2F). Overall, monocyte and B cell frequencies slightly increased after the first vaccination (T2), whereas T cells and NK cells decreased, though without statistical significance.

Monocytes subset dynamics following COVID-19 vaccination in pregnancy

Monocytes are key effector cells of the innate immune system. Previous studies have shown that they act as major drivers of inflammation during COVID-19 infection, particularly $CD14^+$ classical monocytes [11]. Monocytes were further classified into classical monocyte_1 (cM_1), classical monocyte_2 (cM_2), classical monocyte_3 (cM_3) and nonclassical monocytes (ncM) based on transcriptional profiles (Figs. 3A and S2A–B). All classical subsets highly expressed *CD14*, whereas ncM expressed *FCGR3A (CD16)*. Amongst them, cM_1 showed strong expression of proinflammatory genes (*IL1B*, *NLRP3* and *NFKB1*), which suggested a highly activated phenotype; cM_3 expressed immediate early genes (*FOS*, *JUN*, *EGR1* and *IER2*) related to stimulation and signal transduction (Fig. 3B). Figure 3C shows the expression of these key genes in UMAP, where cM_1 formed a cluster enriched for *IL1B*, *NLRP3* and *NFKB1*, whereas *TGFB1* showed no significant difference between subgroups.

To assess immune dynamics after vaccination, monocyte proportions were compared across timepoints. The total proportion of classical monocytes showed no major change; however, cM_1 increased at T2 and returned to baseline (T1) by T3 (Figs. 3D, E and S2C). To explore subset function, GSVA enrichment analysis was performed (Fig. 3F): cM_1 was the main inflammatory effector

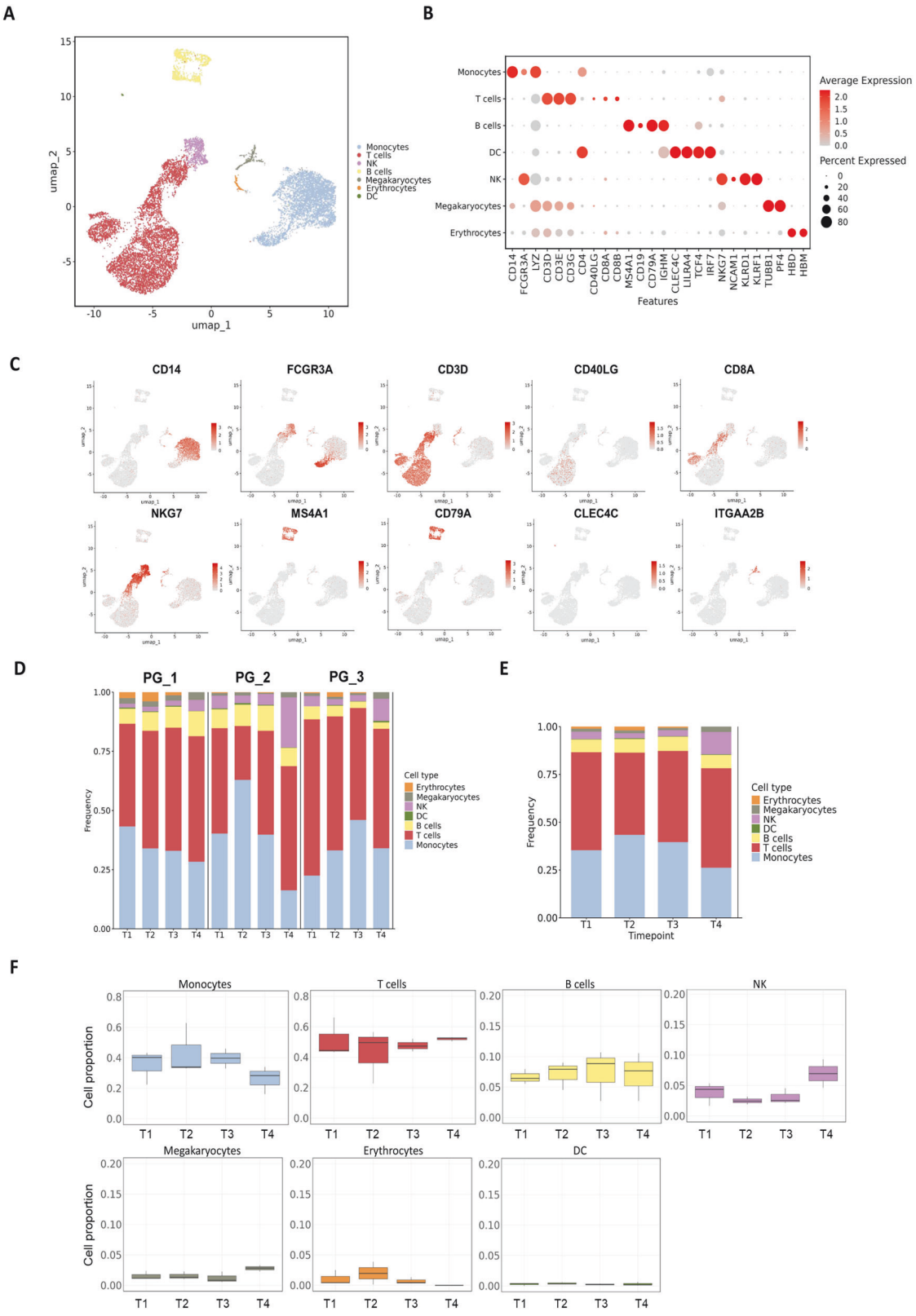

subset enriched in inflammatory and T cell activation pathways; cM_2 expressed *RPS/RPL* genes with stable antimicrobial and metabolic features; and cM_3 was enriched in MAPK, cAMP and TGF-β pathways, representing an AP-1–driven early-sensing subset involved in immune modulation. Differential expression and GO analysis comparing T2 with T1 classical monocytes (Fig. 3H, I) revealed enrichment in lymphocyte differentiation, TGF-β response, steroid hormone response and GPCR signalling regulation, which suggested that monocytes after the first vaccine dose mainly participated in metabolic regulation and immune

Fig. 2 Single-cell immune atlas and composition dynamics of PBMCs in pregnant individuals following COVID-19 vaccination. A UMAP visualisation of single-cell transcriptomes from PBMCs collected at all timepoints from pregnant individuals, annotated by major immune cell types. Each dot represents one cell. **B** Dot plot showing the expression of canonical marker genes for each identified immune cell type. Dot size indicates the percentage of cells expressing the gene, and colour intensity reflects the average expression level. **C** UMAP showing the expression of representative marker genes for major immune cell types in PBMCs, including monocytes (*CD14* and *FCGR3A*), T cells (*CD3D*, *CD8A* and *CD40LG*), NK cells (*NKG7*), B cells (*MS4A1* and *CD79A*), dendritic cells (*CLEC4C*) and platelets (*ITGA2B*). Colour indicates expression level. **D** Bar plots summarising the relative abundance of each immune cell type across timepoints for individual donors. **E** Average cell type composition across all pregnant donors. **F** Box plots quantifying the proportions of each major immune cell type across timepoints. No significant differences were observed between timepoints for any major cell population.

coordination without a strong inflammatory response. This outcome aligns with reports that the first vaccine dose induces immune priming, whereas robust inflammation or humoral responses typically follow the second dose [9, 12]. Overall, in pregnant women, the first COVID-19 vaccine dose caused a transient rise in inflammatory cM_1 cells one week postvaccination, but the overall monocyte response remained moderate.

At T4, the cM_1 population was largely replaced by cM_2 (Figs. 3D and S2D). This sample was collected over a month after the second vaccine dose and delivery. GSVA analysis showed that whilst cM_2 retained partial cM_1-like functions, it lacked several pathways, including the PCSK9–LDLR complex, endosomal vesicle fusion, sphingolipid catabolism, BCL3/10 complex and transmembrane leucine import, all related to lipid metabolism and inflammatory signalling. Dot plots showed lower *IL1B*, *NLRP3* and *NFKB1* expression in cM_2. GO analysis further indicated that compared with T4, T3 displayed stronger responses to viruses, inflammation and lymphocyte adhesion (Fig. S2F–G). Although vaccine-induced responses may persist, pregnancy-associated immune remodelling exerts a stronger effect. After delivery, monocytes likely shifted towards a restorative state and emphasised immune regulation, metabolism and tissue repair.

T cell characteristics following COVID-19 vaccination in pregnancy

To examine T cell subset changes after COVID-19 vaccination in pregnant donors, T/NK cells were classified into eight subtypes: three $CD4^+$ T cell subsets (*CD3D*$^+$, *CD3E*$^+$, *CD4*$^+$ and *CD40LG*$^+$), three $CD8^+$ T cell subsets (*CD3D*$^+$, *CD3E*$^+$, *CD8A*$^+$ and *CD8B*$^+$), one NKT subset (*CD3D*$^+$, *CD3E*$^+$ and *NKG7*$^+$) and one NK subset (*NKG7*$^+$ and *NCAM1*$^+$). The $CD4^+$ subsets comprised CD4_Naive_FHIT, CD4_Tcm_AQP3 and CD4_Tem_CXCL8; the $CD8^+$ subsets included CD8_Naive_LINC02446, CD8_Naive_S100B and CD8_Teff_GZMK (Figs. 4A, B and S3A, B). The UMAP plot showed expression patterns of key genes (*CD4*, *CD8A*, *CD8B*, *CCR7*, *NKG7*, *GZMK*, *GNLY* and *GZMA*) across subsets (Fig. 4C). Analysis of T cell composition over time revealed that T/NK cell proportions remained stable after the first vaccine dose (T2 and T3; Figs. 4D and S3D). According to previous studies, after SARS-CoV-2 mRNA vaccination, naive T cells gradually differentiated into Tcm and Tem subsets, and $CD4^+$ Tcm is recognised as the primary source of long-term immunological memory [9]. Analysis of T cell composition over time revealed that T/NK cell proportions remained stable after the first vaccine dose (T2 and T3; Figs. 4D and S3D). Consistent with previous studies, naive T cells differentiated into Tcm and Tem subsets, and $CD4^+$ Tcm served as a major source of long-term memory. Although changes in CD4_Tcm_AQP3 (increased) and CD4_Naive_FHIT (decreased) were not statistically significant, the trend aligns with reported postvaccination differentiation dynamics. Functional activity assessed by GSVA showed that except for quiescent CD4_Naive_FHIT, all other subsets (CD4_Tcm_AQP3, CD4_Tem_CXCL8, CD8_Naive_LINC02446 and CD8_Naive_S100B) exhibited activation of pathways such as dendritic cell dendrite assembly, CCL19/21 signalling and lymphoid lineage migration. NK, NKT and CD8_Teff_GZMK subsets were enriched in immune and eosinophil activation pathways. Notably, NK and NKT cells also showed upregulation of killer-cell immunoglobulin-like receptor and MHC class Ib inhibitory receptor pathways, which suggest regulatory cytotoxic and antigen-recognition potential.

To examine functional changes in T cells further, DEGs and enriched Gene Ontology (GO) pathways at T2 and T3 were analysed and compared with T1 (Fig. 4G and H). In the T2 versus T1 comparison, several genes involved in T cell activation and metabolism (e.g. *RPS26*, *LEPROTL1*, *CREM* and *ICOS*) were significantly upregulated, along with enrichment of pathways related to CD4-positive alpha–beta T cell activation, T cell proliferation and leukocyte adhesion. These results suggest that shortly after vaccination, T cells undergo robust activation and initiation of immune responses, primarily driven by $CD4^+$ T cells. At T3, T cells displayed a distinct transcriptional profile enriched for pathways associated with apoptosis, energy metabolism, redox regulation and mitochondrial activity. Collectively, these findings indicate that even during pregnancy, mRNA vaccination effectively induces T cell activation and differentiation, and T cells gradually transition into functionally mature or memory-maintaining states over time.

Compared with the DEGs identified before delivery (T2 versus T1 and T3 versus T1), the T3 versus T4 comparison revealed more DEGs. Because T4 represents the stage after the second vaccination and delivery, these immune alterations likely reflect combined effects. Besides increases in CD4_Tem_CXCL8 and cytotoxic subsets (NK, NKT and CD8_Teff_GZMK), most T cell subsets declined in proportion, and CD4_Tem_CXCL8 reached statistical significance (Fig. S3D). At the transcriptional level, T3 and T4 T cells showed distinct expression profiles (Fig. S3E). GO enrichment analysis indicated that T3 cells were enriched in T cell differentiation, RNA splicing and lymphocyte differentiation pathways and reflected higher activation than T4. By contrast, T4 cells were enriched in aerobic respiration, mitochondrial metabolism, oxidative phosphorylation and ATP synthesis, which suggested a metabolic shift towards greater energy demand, possibly compensating for the immunosuppressive state of pregnancy (Fig. S3F).

Changes in B cell following COVID-19 vaccination during pregnancy

B cells play a central role in vaccine-induced immunity by mediating humoral responses and establishing immune memory. In our analysis, B cells were regrouped into four clusters and classified into three main subtypes based on canonical markers: Naive_B, Memory_B_GRP183 and Memory_B_ITGB1 (Figs. 5A, B and S4A–B). UMAP visualisation revealed subtype-specific expression: Naive B cells expressed *TCL1A*, *IGHD* and *MEF2C*; memory B cells expressed *CD27* and *TNFRSF13B*; and *XBP1* marking plasma cell differentiation, although no plasma cells were detected (Fig. 5C). Composition analysis showed that B cell subset proportions remained stable across T1–T3 (Figs. 5D, E and S4C). To explore functional heterogeneity, GSVA was performed and showed that Naive B cells displayed low activity across most pathways, except modest enrichment in IgM complex and low-affinity IgE receptor genes. By contrast, Memory_B_ITGB1 was

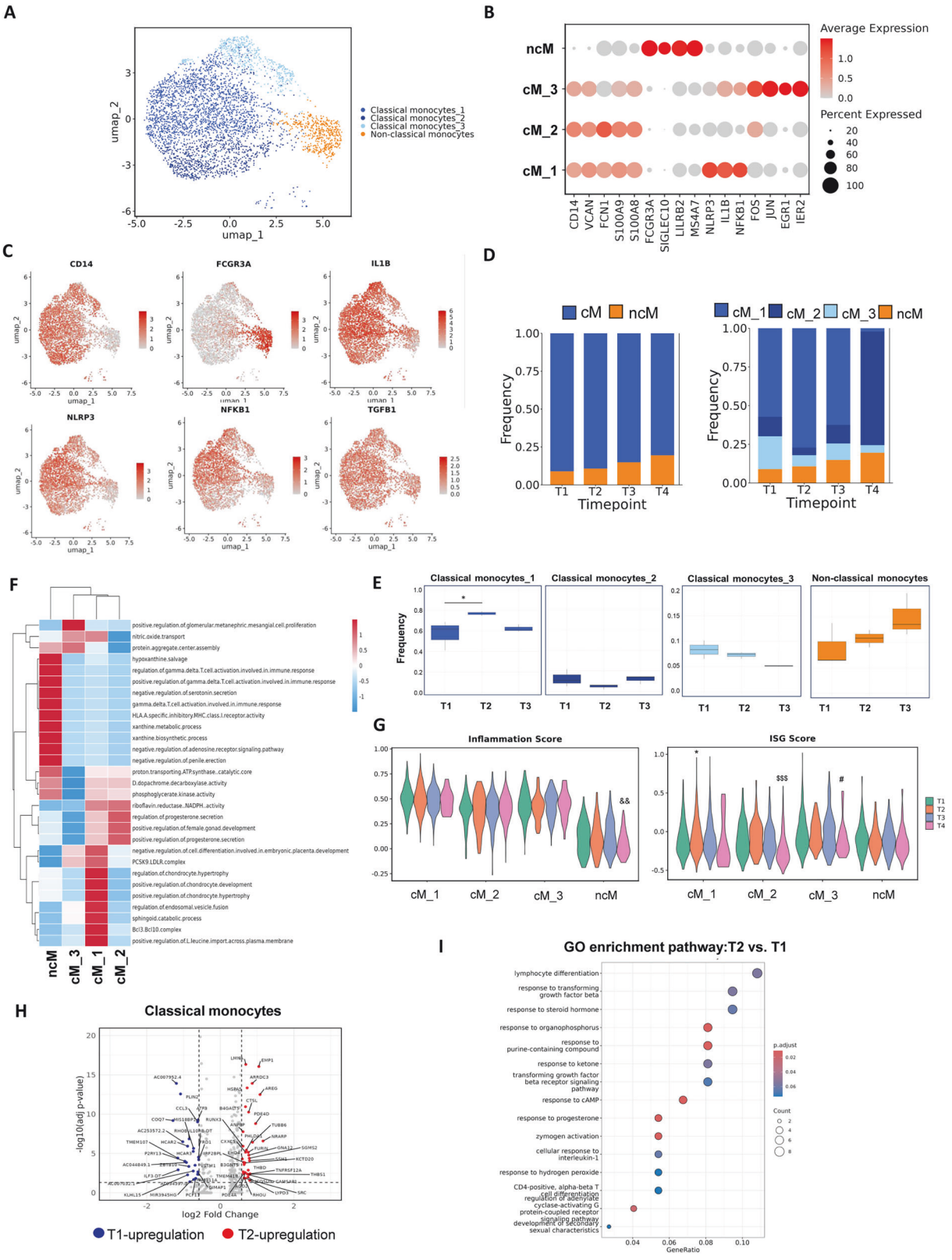

enriched in pathways related to lipid metabolism and immune regulation (e.g. PCSK9–AnxA2 complex and glucocorticoid catabolic process), TLR1/TLR2 signalling and cellular migration (uropod and trailing edge membranes). Memory_B_GRP183 showed similar but slightly weaker activation (Fig. 5F).

Unlike monocytes and T cells, which exhibited transcriptional changes as early as T2, B cells showed no significant DEGs at T2 or T3 (Fig. 5G). This result aligns with antibody data showing major increases in anti–SARS-CoV-2 IgG only after the second vaccine dose, which suggested minimal B cell response after the first dose.

Fig. 3 Transcriptional heterogeneity and dynamic changes of monocyte subsets following COVID-19 vaccination in pregnancy. A UMAP showing transcriptional subclusters of monocytes from PBMCs across all timepoints. **B** Dot plot showing key marker genes for classical and nonclassical monocytes. **C** UMAP plots displaying representative marker genes and inflammation-related gene expression across monocyte subsets. **D** Stacked bar plots showing the proportions of cM and ncM (left) and further resolution of classical monocyte subclusters (cM_1, cM_2 and cM_3; right) across four timepoints (T1–T4). **E** Box plots showing the frequency of each monocyte subcluster over time. *$p < 0.05$ compared with T1, Wilcoxon rank-sum test. **F** Gene set variation analysis (GSVA) showing differential pathway activity across monocyte subclusters. **G** Violin plots showing inflammation and ISG scores across subsets using AddModuleScore. Symbols indicate significant changes versus T1 in each subset: *cM_1, $cM_2, #cM_3 and &ncM. **H** Volcano plot showing DEGs between T2 and T1 within cMs. **I** GO enrichment analysis of DEGs between T2 and T1 in cMs.

Comparison of T3 versus T4 reflected the effects of delivery and the second dose and showed minor but nonsignificant shifts in B cell subset proportions (Fig. S4D). DEG and GO analyses of memory B cells revealed T3 enrichment in oxidative stress and metabolic pathways (e.g. response to hydrogen peroxide and reactive oxygen species), which suggested a primed effector state. By T4, memory B cells exhibited reduced transcriptional activity and likely reflected postdelivery recovery (Figs. S4E, F).

DISCUSSION

Pregnant individuals face an increased risk of severe illness and mortality from COVID-19, and this prompted the CDC to recommend vaccination during pregnancy. However, early data were limited and left uncertainties about vaccine safety and efficacy in this population. Subsequent systematic reviews have reported no association between COVID-19 vaccination and adverse maternal or neonatal outcomes. To address remaining knowledge gaps, this study employed 10x Genomics scRNA-seq to investigate immune cell composition and transcriptional changes during pregnancy following COVID-19 vaccination. Whilst moderate immune modulation was observed, the response was less pronounced than that induced by infection and largely resembled that of nonpregnant individuals after vaccination [13, 14].

Through single-cell transcriptomic profiling, this study revealed distinct immune dynamics in pregnant women during vaccination. After the first vaccine dose, innate immune activation was evident, marked by a transient increase in proinflammatory monocytes (cM_1), yet the overall immune response remained controlled, without excessive inflammation or ISG activation. T cells exhibited activation, proliferation and differentiation and progressively transitioned into memory and functionally mature subsets, likely driven by $CD4^+$ T cells. By contrast, the first dose appeared insufficient to elicit a strong B cell response; a marked rise in antibody levels and transcriptional activity was observed only after the second dose. Postpartum samples indicated a shift towards pathways associated with metabolic regulation and tissue repair and underscored the adaptive interplay between vaccination and childbirth. Overall, pregnant women were still capable of generating effective antibody responses after vaccination and delivery. The antibody levels observed after the second dose were markedly higher than those after the first dose, which indicated that neither pregnancy nor delivery impaired the ability to mount a humoral immune response. This pattern is consistent with findings from previous studies in the general population showing enhanced antibody responses following the second vaccine dose [15].

Despite providing valuable insights into the immune response to COVID-19 vaccination during pregnancy, this study has several limitations. Firstly, the sample size was limited to three pregnant participants, which constrained the generalisability of the findings and limits assessment of inter-individual variability. Secondly, cell damage from cryopreservation resulted in suboptimal cell recovery in some samples. The reduced cell numbers may have limited the detection of rare or transient immune subsets and underestimated certain responses. Thirdly, the final timepoint (T4) was collected after the second vaccine dose and childbirth, which hindered distinguishing whether the observed immune changes were primarily driven by vaccination or by physiological effects of delivery. Nevertheless, the results were carefully interpreted within these constraints to provide the most accurate representation of the available data.

Early innate immune activation patterns consistent with the results of two previous scRNA-seq studies in healthy individuals were observed. Wang et al. [16] showed an increase in $CD14^+$ monocytes following BNT162b2 mRNA vaccination, accompanied by upregulation of *ISGs* and inflammatory genes such as *IL1B*, *TNF* and *NFKBIA*. These observations align with our identification of the cM_1 monocyte subset in pregnant individuals, which was enriched at T2 and characterised by elevated expression of *IL1B*, *NLRP3* and *NFKB1*, as well as higher *ISG* activity. Similarly, both studies reported activation and differentiation of $CD4^+$ T cells into memory-like subsets after the first vaccine dose, which suggested that adaptive T cell responses remained functionally intact despite the immunoregulatory milieu of pregnancy.

By contrast, a study by Tong et al. [9] analysing immune responses to the BBIBP-CorV inactivated vaccine in healthy individuals revealed more distinct patterns. Although both studies reported an early increase in proinflammatory monocytes after vaccination, the response in our pregnant cohort appeared more transient and lacked strong *ISG* activation, which may be attributable to the limited sample size. Tong et al. further observed sustained activation of $CD14^+$ and $CD16^+$ monocytes, along with upregulation of type I interferon and toll-like receptor (TLR) signalling pathways, which indicated a more pronounced innate immune response. Whilst both studies consistently observed $CD4^+$ T cell activation, B cell responses diverged: Significant transcriptional activation or antibody production were not detected from B cells at T2 and T3, whereas BBIBP-CorV recipients showed plasma cell expansion and BCR recombination at comparable time points. These differences likely reflected the distinct vaccine platforms (mRNA versus inactivated) and the unique immunological state of pregnancy.

Aghaeepour et al. [17] previously reported that the frequency of B cells and the expression of their activation markers are significantly reduced during pregnancy, particularly in the third trimester, which indicates an overall suppression of humoral immunity [18]. This hypoactive B cell state contributes to maternal–foetal immune tolerance and prevents excessive antibody-mediated inflammatory responses. In this study, this immunosuppressive environment may explain the lack of a robust B cell response following the first vaccine dose. Overall, these findings highlight the importance of considering gestational immune dynamics when evaluating vaccine-induced responses in pregnant individuals.

To our knowledge, this study represents the only single-cell transcriptomic investigation of immune dynamics in pregnant individuals receiving COVID-19 vaccination. Whilst previous studies relied primarily on serological data or bulk RNA analyses, our work, though limited by a small sample size, still revealed unique immune dynamics. Longitudinal analysis across multiple timepoints showed that pregnant individuals can mount a coordinated T cell response and display transient activation of proinflammatory monocytes, whilst the B cell response appears

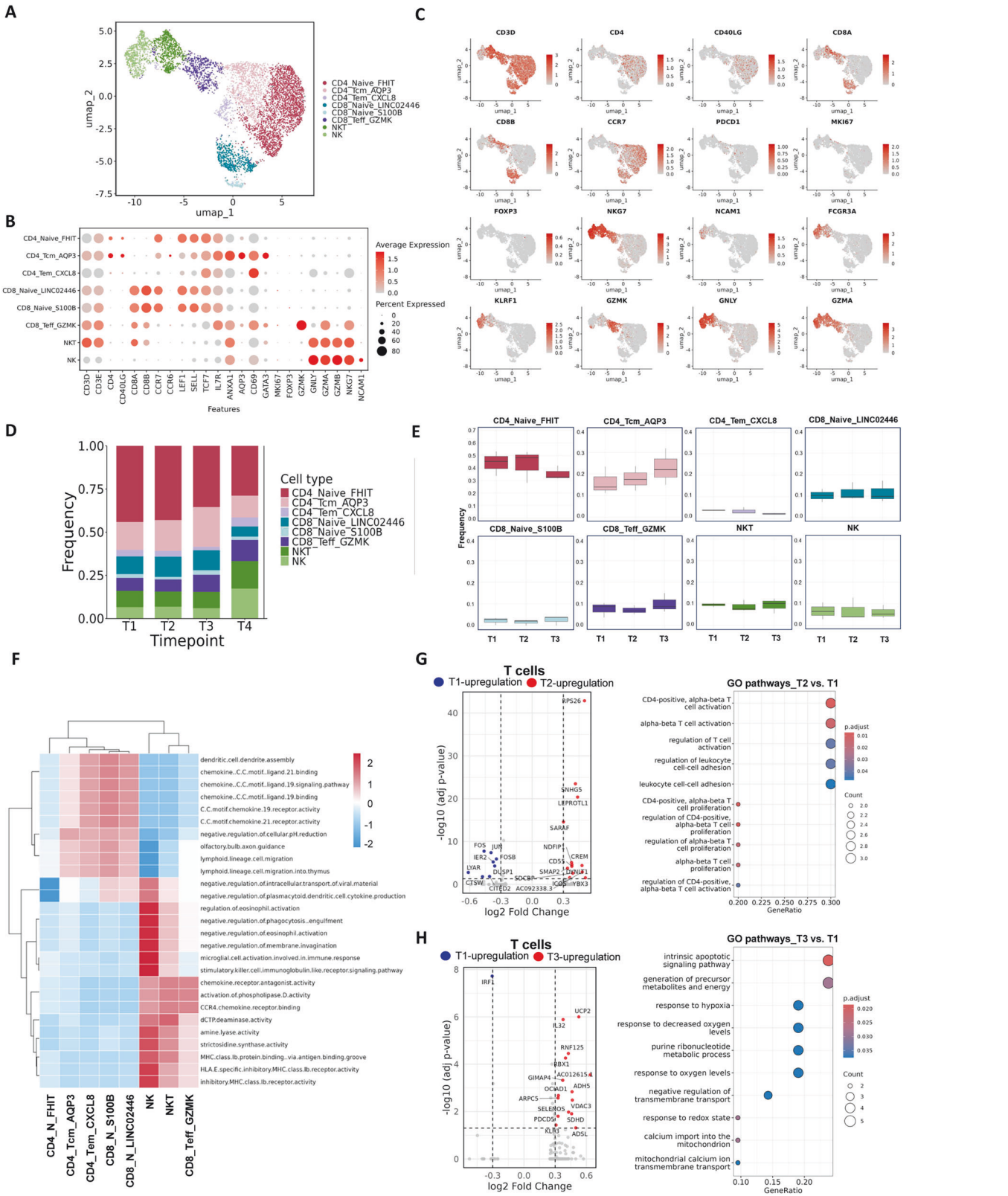

Fig. 4 Changes in T cell and NK cell subsets after COVID-19 vaccination during pregnancy. A UMAP visualisation of T cell and NK cell subsets from PBMCs across all timepoints. **B** Dot plot showing the expression of key marker genes for T cell and NK cell subsets. **C** UMAP plots displaying representative genes for T cell and NK cell populations. Markers include pan-T cell (*CD3D*), CD4⁺ T cell (*CD4* and *CD40LG*), CD8⁺ T cell (*CD8A* and *CD8B*), memory/naive T cell (*CCR7*), regulatory T cell (*FOXP3*), proliferation (*MKI67*), exhaustion (*PDCD1*), NK cell (*NKG7*, *NCAM1*, *FCGR3A* and *KLRF1*) and effector cytotoxic markers (*GZMK*, *GNLY* and *GZMA*). **D** Bar plot showing the average proportion of each subset across all timepoints. **E** Box plots quantifying the proportions of all subsets across timepoints. **F** GSVA showing differences in pathway activity amongst T cell and NK cell subsets. **G** Volcano plot and GO enrichment analysis of DEGs in all T cells comparing T2 with T1. **H** Volcano plot and GO enrichment analysis of DEGs in all T cells comparing T3 with T1.

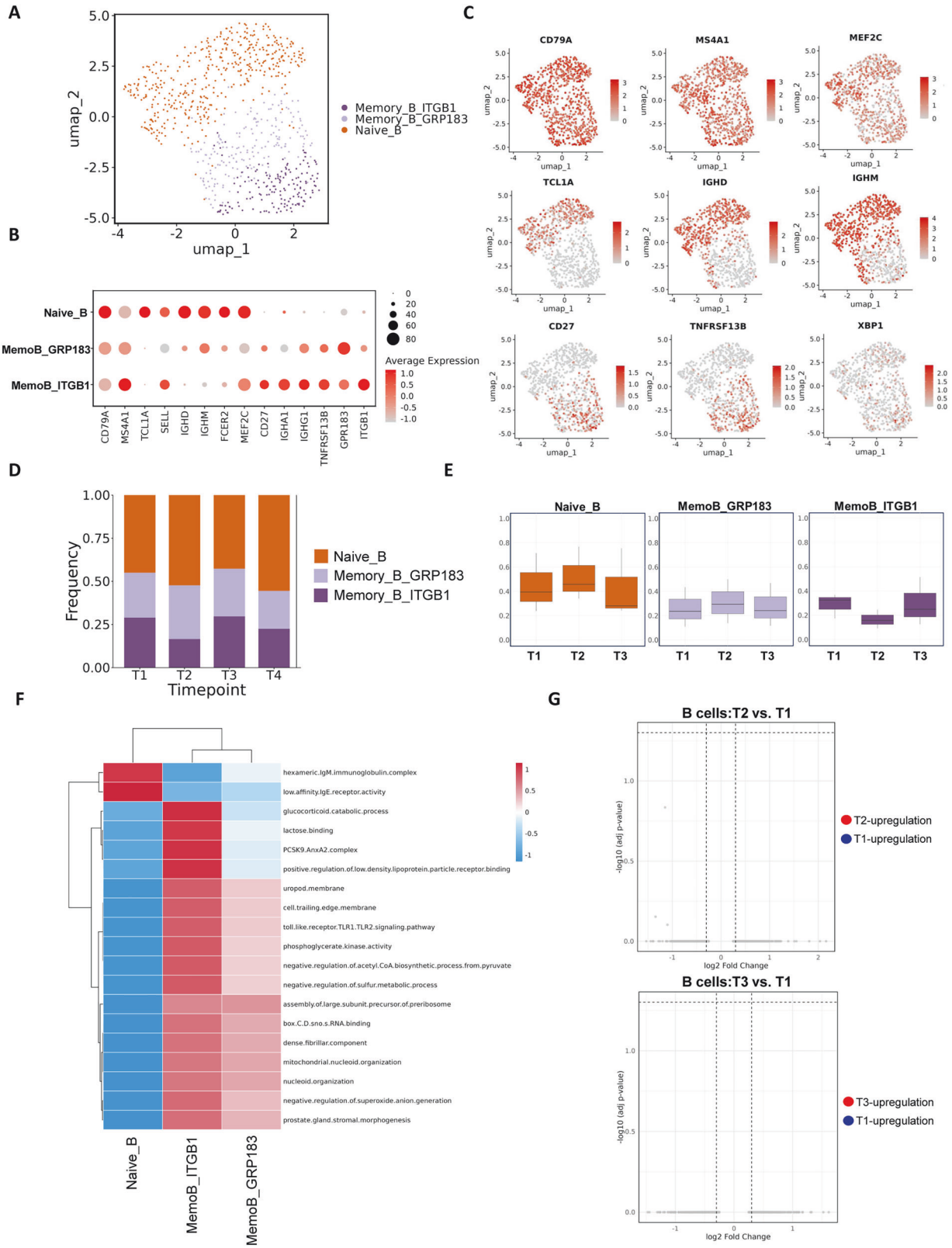

Fig. 5 Transcriptional and compositional changes in B cell subsets after COVID-19 vaccination during pregnancy. A UMAP showing B cell subsets across all timepoints. **B** Dot plot of marker gene expression in each B cell subset. **C** UMAP plots showing the expression of key B cell–related genes, including canonical markers (*CD79A* and *MS4A1*), transcription factors (*MEF2C* and *XBP1*), activation/proliferation markers (*TCF4*, *CD27* and *TNFRSF13B*) and immunoglobulin genes (*IGHG1*, *IGHM* and *IGHD*). **D** Bar plot showing the proportion of each B cell subset over time. **E** Box plots showing changes in subset frequency. **F** Heatmap showing GSVA pathway differences between B cell subsets. **G** Volcano plots showing DEGs in B cells comparing T2 versus T1 (top) and T3 versus T1 (bottom).

delayed or attenuated. These findings underscore the unique immunological landscape of pregnancy and provide mechanistic support for current public health recommendations on COVID-19 vaccination during pregnancy. Notably, our data indicate that mRNA vaccination induced immune memory without excessive inflammation, which reinforces its safety and potential efficacy as part of antenatal immunisation strategies.

DATA AVAILABILITY

The datasets used in this research are available at https://zenodo.org/records/13969283.

CODE AVAILABILITY

The data and code that support the findings of this study are available from the corresponding author, upon reasonable request.

REFERENCES

1. WHO. WHO Coronavirus (COVID-19) Dashboard. 2023.
2. Pregnant and Recently Pregnant People. *Centers for Disease Control and Prevention*. https://www.cdc.gov/coronavirus/2019-ncov/need-extra-precautions/pregnant-people.html#anchor_1614966846976 2022.
3. Taylor MM, Kobeissi L, Kim C, Amin A, Thorson AE, Bellare NB, et al. Inclusion of pregnant women in COVID-19 treatment trials: a review and global call to action. Lancet Glob Health. 2021;9:e366–e371.
4. Villar J, Ariff S, Gunier RB, Thiruvengadam R, Rauch S, Kholin A, et al. Maternal and Neonatal Morbidity and Mortality Among Pregnant Women With and Without COVID-19 Infection: The INTERCOVID Multinational Cohort Study. JAMA Pediatr. 2021;175:817–26.
5. Allotey J, Stallings E, Bonet M, Yap M, Chatterjee S, Kew T, et al. Clinical manifestations, risk factors, and maternal andperinatal outcomes of coronavirus disease 2019 in pregnancy: living systematic review and meta-analysis. BMJ 2020;370:m3320.
6. Moro PL, Olson CK, Clark E, Marquez P, Strid P, Ellington S, et al. Post-authorization surveillance of adverse events following COVID-19 vaccines in pregnant persons in the vaccine adverse event reporting system (VAERS), December 2020 - October 2021. Vaccine. 2022;40:3389–94.
7. Sadarangani M, Soe P, Shulha HP, Valiquette L, Vanderkooi OG, Kellner JD, et al. Safety of COVID-19 vaccines in pregnancy: a Canadian National Vaccine Safety (CANVAS) network cohort study. Lancet Infect Dis. 2022;22:1553–64.
8. Wen W, Su W, Tang H, Le W, Zhang X, Zheng Y, et al. Immune cell profiling of COVID-19 patients in the recovery stage by single-cell sequencing. Cell Discov. 2020;6:31.
9. Tong R, Luo L, Zhao Y, Sun M, Li R, Zhong J, et al. Characterizing the cellular and molecular variabilities of peripheral immune cells in healthy recipients of BBIBP-CorV inactivated SARS-CoV-2 vaccine by single-cell RNA sequencing. Emerg Microbes Infect. 2023;12:e2187245.
10. Chen D, Wang W, Wu L, Liang L, Wang S, Cheng Y, et al. Single-cell atlas of peripheral blood mononuclear cells from pregnant women. Clin Transl Med. 2022;12:e821.
11. Ren X, Wen W, Fan X, Hou W, Su B, Cai P, et al. COVID-19 immune features revealed by a large-scale single-cell transcriptome atlas. Cell. 2021;184:5838.
12. Sahin U, Muik A, Derhovanessian E, Vogler I, Kranz LM, Vormehr M, et al. COVID-19 vaccine BNT162b1 elicits human antibody and T(H)1 T cell responses. Nature. 2020;586:594–9.
13. Ciapponi A, Berrueta M, Argento FJ, Ballivian J, Bardach A, Brizuela ME, et al. Safety and Effectiveness of COVID-19 Vaccines During Pregnancy: A Living Systematic Review and Meta-analysis. Drug Saf. 2024;47:991–1010.
14. Shafiee A, Kohandel Gargari O, Teymouri Athar MM, Fathi H, Ghaemi M, Mozhgani SH. COVID-19 vaccination during pregnancy: a systematic review and meta-analysis. BMC Pregnancy Childbirth. 2023;23:45.
15. Matsuura T, Fukushima W, Nakagama Y, Kido Y, Kase T, Kondo K, et al. Factors impacting antibody kinetics, including fever and vaccination intervals, in SARS-CoV-2-naive adults receiving the first four mRNA COVID-19 vaccine doses. Sci Rep. 2024;14:7217.
16. Wang Y, Wang X, Luu LDW, Li J, Cui X, Yao H, et al. Single-cell transcriptomic atlas reveals distinct immunological responses between COVID-19 vaccine and natural SARS-CoV-2 infection. J Med Virol. 2022;94:5304–24.
17. Lima J, Martins C, Leandro MJ, Nunes G, Sousa MJ, Branco JC, et al. Characterization of B cells in healthy pregnant women from late pregnancy to post-partum: a prospective observational study. BMC Pregnancy Childb. 2016;16:139.
18. Liu JC, Zeng QX, Duan YG, Yeung WSB, Li RHW, Ng EHY, et al. B cells: roles in physiology and pathology of pregnancy. Front Immunol 2024;15:1456171.

FUNDING

This research was funded by grants NSTC 111-2314-B-005 -007 -MY3 from the National Science and Technology Council, Taiwan. Open access funding provided by Taichung Veterans General Hospital.

COMPETING INTERESTS

The authors declare no competing financial interests.

ETHICS APPROVAL AND CONSENT TO PARTICIPATE

This study was approved by the Institutional Review Board of Taichung Veterans General Hospital (IRB No. CF21270A). All methods were performed in accordance with the relevant guidelines and regulations. Written informed consent was obtained from all participants prior to sample collection.

ADDITIONAL INFORMATION

Supplementary information The online version contains supplementary material available at https://doi.org/10.1038/s41435-026-00394-2.

Correspondence and requests for materials should be addressed to Yi-Ming Chen or Tzu-Hung Hsiao.